1 The limited contribution of early visual cortex in visual working memory for surface roughness

2 (Abbreviated title: fMRI decoding surface roughness in VWM)

3 Munendo Fujimichi[1,2], Hiroki Yamamoto[1], and Jun Saiki[1]

4 [1]Graduate School of Human and Environmental Studies, Kyoto University, Yoshida-Nihonmatsucho, Sakyo-ku,

5 Kyoto 606-8501, Japan

6 [2]Japan Society for the Promotion of Science, Tokyo, Japan

7 Corresponding author email address: fujimichi@cv.jinkan.kyoto-u.ac.jp

Abstract

9   Are visual representations in the human early visual cortex necessary for visual working memory
10 (VWM)? Previous studies suggest that VWM is underpinned by distributed representations across
11 several brain regions, including the early visual cortex. Notably, in these studies, participants had to
12 memorize images under consistent visual conditions. However, in our daily lives, we must retain the
13 essential visual properties of objects despite changes in illumination or viewpoint. The role of brain
14 regions—particularly the early visual cortices—in these situations remains unclear. The present
15 study investigated whether the early visual cortex was essential for achieving stable VWM. Focusing
16 on VWM for object surface properties, we conducted fMRI experiments while male and female
17 participants performed a delayed roughness discrimination task in which sample and probe spheres
18 were presented under varying illumination. By applying multi-voxel pattern analysis to brain activity
19 in regions of interest, we found that the ventral visual cortex and intraparietal sulcus were involved
20 in roughness VWM under changing illumination conditions. In contrast, VWM was not supported as
21 robustly by the early visual cortex. These findings show that visual representations in the early visual
22 cortex alone are insufficient for the robust roughness VWM representation required during changes
23 in illumination.

24 Keywords: roughness, visual working memory, fMRI, early visual cortex

Declarations

Acknowledgements

Note

The final publication is available at

Introduction

Visual working memory (VWM) plays an important role in cognition. Functional brain imaging studies employing univariate analysis have revealed that brain activation in the intraparietal sulcus (IPS) reflected maintenance of spatial information in visual short-term memory (VSTM; Harrison et al. 2010; Todd & Marois 2004, 2005; Ungerleider et al. 1998; Xu & Chun 2006). Studies using multi-voxel pattern analysis (MVPA) have shown that multiple brain regions contribute to VWM. In particular, the early visual cortex may play a role in orientation (Harrison & Tong 2009), contrast (Xing et al. 2013), and color pattern elements (Christophel et al. 2012) of VWM. In these studies, participants were asked to memorize an image under set visual conditions; however, our daily lives necessitate retention of the essential properties of objects against changes despite changes in visual conditions, such as illumination and viewpoint. The role of specific brain regions, especially the early visual cortices, under changing visual conditions remains unclear.

To address this issue, we focused on object surface properties, such as glossiness and roughness, that humans can perceive despite changes in the illumination of visual images (Fleming et al. 2003; for a review, see Komatsu & Goda 2018; Tsuda & Saiki 2018). The ventral visual pathway has a vital role in material perception, whereas the early visual cortex has a limited role. The early visual cortices can compute low-level image features, such as luminance skewness, to estimate object surface qualities (Cant et al. 2009; Motoyoshi et al. 2007; Sun et al. 2015; Wada et al. 2014). Although computation alone is insufficient to achieve material perception, this process may be a necessary component (Hiramatsu et al. 2011). Regarding VWM for illumination-invariant material properties, illumination-invariant ventral representation may need to be accompanied by representation in the early visual cortex to retain stability (Christophel et al. 2017). Unlike material perception with online visual input, VWM without visual input may require interaction between the ventral visual pathway and early visual cortex to maintain a stable representation. Alternatively, only illumination-invariant surface properties may be maintained in the ventral visual pathway, and representation in the early visual cortex may be discarded to avoid confusion due to changes in visual images between memorized and test stimuli.

Numerous studies without visual interference during maintenance of visual features have reported memory representations in the early visual cortex. A recent study showed that visual distractors during VWM maintenance disrupted representations in the early visual cortex (Bettencourt & Xu 2016). However, this finding alone is insufficient to conclude that the early visual cortex is not involved in retaining stable VWM representations. For instance, there may be apparent reduction in decoding performance due to increased neuronal response to task-irrelevant visual distractors. Thus, it remains unclear whether the early visual cortex is involved in maintaining VWM that is robust against changes in illumination and viewpoint. It is important to examine whether anticipation of visual image changes in a test stimulus are sufficient to discard the representation within the early

76 visual cortex to elucidate the nature of distributed VWM representations.

77 To address these questions, we focused on the surface property of roughness. We conducted an

78 experiment using a delayed roughness discrimination task in which sample and probe objects were

79 rendered in different illuminations. To cope with the different illumination, we hypothesized that the

80 visual system would establish an illumination-invariant roughness representation for VWM in lieu of

81 an image-based representation in the early visual cortex. We applied MVPA to brain activity specific

82 to VWM from the ventral visual pathway, early visual cortex, and IPS during a delay period. If

83 illumination-invariant representation of roughness alone can be selectively maintained, we expected

84 that the ventral visual cortex and IPS, but not early visual cortex, would be involved in roughness

85 VWM. Alternatively, if roughness VWM requires a distributed representation of image-based and

86 illumination-invariant information, we expected that the early visual cortex in addition to the ventral

87 visual cortex and IPS would be involved.

88

Materials and Methods

89

Participants

90

91 Twenty-four undergraduate and graduate students with no history of psychiatric or neurological

92 diseases participated in a visual working memory experiment, a functional localization scan, and a

93 retinotopy scan (8 women; mean age = 22.04 years). All participants had normal color vision,

94 confirmed by an Ishihara test, as well as normal or corrected-to-normal vision acuity with

95 non-magnetic glasses. Participants viewed stimuli monocularly with the left eye while vision in the

96 right eye was obstructed by inserting a black mask in the right lens of the glasses. Monocular

97 viewing was employed to prevent double vision caused by a head coil shielding a major portion of

98 the binocular visual field. After receiving a detailed description of the study, all participants provided

99 written informed consent. The experiment was conducted in accordance with the guidelines of the

100 Ethical Committee of the Graduate School of Human and Environmental Studies at Kyoto

101 University. All participants received a book coupon (5000 Japanese yen) for their participation.

102

Visual working memory experiment

103

Stimuli

104

105 Computer-generated three-dimensional spheres, similar to those used in a previous behavioral study

106 (Tsuda & Saiki 2018), were used as sample and probe stimuli. The surface appearance of the sample

107 spheres was set at one of two different levels of roughness with jitters (Fig. 1). The sharpness

108 parameter (α) for each level of roughness was 0.016667 ($\pm$0.001667) and 0.080000 ($\pm$0.001667),

109 respectively while glossiness (specular reflectance parameter; ρ_s) was maintained at 0.040617. The α

110 and ρ_s parameters were controlled using RADIANCE (Ward 1994). For probe spheres, three

111 different levels of roughness were rendered in a similar way; the levels of roughness were 0.003333

4

112   (±0.001667), 0.040000 (±0.001667), and 0.098333 (±0.001667), respectively, with glossiness

113   maintained at 0.040617. All spheres were rendered in two different real-world illuminations derived

114   from Debevec (1998): 'Kitchen' and 'Overcast Breezeway'.

115

116   **Procedure**

117   In the VWM experiment, participants performed a delayed roughness discrimination task. A sample

118   of the trial design is shown in Figure 2. Each trial began with two samples (10.3° × 10.3°) presented

119   sequentially for 500 ms each. A black cross (1.2° × 1.2°) was displayed for 500 ms between the two

120   samples. The sample stimuli consisted of one rough sphere and one smooth sphere. Following the

121   two samples, a numerical cue (1 or 2; 1.9° × 3.4°) was displayed, indicating which sample should be

122   memorized. After an 11-s delay, a probe sphere was presented and participants were asked to

123   indicate within 2 s whether the probe sphere had higher or lower roughness than the memorized

124   sphere. The illumination contexts of the sample spheres and probe sphere were always different to

125   prevent memorization of the visual image instead of the material properties. Between trials, a black

126   cross was presented for 0–10 s. Each run (144 s) consisted of four trials, plus an initial 14-s black

127   cross presentation that was excluded from analysis. Within each run, the order of rough and smooth

128   samples and the samples sphere to be memorized were counterbalanced. All participants performed

129   10 runs.

130

131   **Functional magnetic resonance imaging (fMRI) data acquisition**

132   This study was conducted using the MRI scanner and related facilities at the Kokoro Research

133   Center, Kyoto University. Data were collected on a 3 T Siemens scanner (3.0 T MAGNETOM Verio).

134   Functional data were obtained with T2*-weighted imaging (repetition time (TR) = 2000 ms; field of

135   view = 224 × 224 mm; voxel size = 3.5 × 3.5 × 3 mm; slice number = 34 slices). T1-weighted

136   anatomical images were also acquired for each participant.

137

138   **fMRI data analysis**

139   **Brain surface reconstruction, preprocessing, and multi-voxel pattern analysis**

140   All fMRI data were analyzed with the supercomputer at the Academic Center for Computing and

141   Media Studies, Kyoto University. We reconstructed the cortical surfaces for each participant from

142   the T1-weighted image volumes. We used the recon-all script in FreeSurfer-6.0.0

143   (surfer.nmr.mgh.harvard.edu/) for gray and white matter segmentation, surface smoothing, and

144   inflation. Preprocessing of fMRI data was performed using Analysis of Functional NeuroImages

145   (AFNI; Cox 1996) and Surface Mapping with AFNI (SUMA; Saad et al. 2004).

146   Accuracy of MVPA for roughness was determined using the following six steps: (1) The fMRI data

147   were corrected for slice timing and head motion with realignment to the first volume. (2) The

148 functional images were registered to the cortical surfaces for each participant. (3) Voxel-based

149 preprocessing, linear trend removal, and percent signal change conversion were applied to the fMRI

150 data. (4) A deconvolution technique (Dale 1999) was applied to the fMRI data, estimating the time

151 course for each rough or smooth memory condition. (5) The deconvoluted signals were sampled

152 within each region of interest (ROI) as described below. (6) MVPA was performed for the signals at

153 each TR using the libsvm-3.20 script (Chang & Lin 2011) in MATLAB 9.1.0 (MathWorks). The

154 leave-one-out cross-validation procedure was used to estimate decoding performance. Learning runs

155 were trained for each TR to create a decoder that could predict the memorized roughness condition

156 based on brain activity patterns. The decoder was then used to predict whether the brain activity

157 pattern in each test run belonged to memorization of the rough or smooth sphere. This procedure was

158 repeated until all runs had been tested, and the resultant roughness classification performance was

159 defined as the MVPA accuracy.

160

161 **Regions of interest**

162 Following the VWM experiment, we performed two types of scans on the left eye of each

163 participants to localize the visual area. The first scan (functional localization scan) localized the

164 higher-order visual areas using natural images in one of the following categories: faces, scenes,

165 objects, and color. In addition, scrambled faces, scrambled scenes, scrambled objects, and gray

166 images were used. These images were collected from open source material databases and websites,

167 including Japanese movie information (faces), Japanese real estate companies (scenes), and car

168 dealers and supermarkets (objects). A block design was used for functional localization scans (Fig. 3).

169 Each run consisted of eight blocks: a face block, a scrambled face block, a scene block, a scrambled

170 scene block, an object block, a scrambled object block, a color block, and a gray block. Within each

171 12-s block, including rest duration (4 s), 16 collages of natural images belonging to a single block

172 condition were presented sequentially for 0.5 s each. Participants pressed a button when each block

173 started. These blocks were conducted in a random order at various intervals between 0–10 s.

174 Intervals were determined pseudo-randomly using optseq2—a FreeSurfer tool for scheduling events

175 (surfer.nmr.mgh.harvard.edu/optseq/). A black cross ($0.9° \times 0.9°$) was presented during the rest

176 intervals. Each run (374 s total) consisted of 24 blocks, plus an initial 14-s black cross presentation

177 that was excluded from analysis. All participants performed three runs.

178 Based on the functional localization scan, we defined freehand ROIs in the left and right ventral

179 visual cortices (Fig. 4a) and left and right IPSs (Fig. 4b) for each participant individually. We

180 selected the left and right ventral visual cortices because they are involved in face-, scene-, object-,

181 and color-processing. To identify these areas, we contrasted the brain activities in response to face vs

182 scrambled face blocks, scene vs scrambled scene blocks, object vs scrambled object blocks, and

183 color vs gray blocks using a standard general linear model (GLM) approach in AFNI (afni_proc

184 function). The fMRI time series of each block condition was modeled by convolving a 16-s boxcar
185 function with a canonical hemodynamic response function. We computed GLM β coefficients of
186 standard AFNI parameters for each voxel, and estimated the contributions of each category (faces,
187 scenes, objects, and color) to the blood oxygen level dependent responses of the voxels in the ventral
188 visual cortex. For the mapping of the results of this comparison, the voxel-wise p-value threshold
189 was set to .001 for faces, scenes, and objects and .01 for color because color selectivity has been
190 shown to be weaker than the selectivity in other categories (Lafer-Sousa et al. 2016). We carefully
191 defined ROIs as the statistically significant (not adjusted) voxel clusters in the visual anatomical
192 brain regions for each participant individually. The average ROI sizes for all participants were as
193 follows: left/right face area = 264/236 voxels, left/right scene area = 142/128 voxels, left/right object
194 area = 205/139 voxels, and left/right color area = 110/113 voxels. These corresponded to a cluster
195 threshold level of α ~ .10 estimated using the 3dClustSim function in AFNI. We defined the left and
196 right face processing related IPSs as the IPS because of the interplay between the IPS and face
197 processing. The parietal cortex, including the IPS, is connected to the posterolateral aspect of the
198 fusiform gyrus (FG) (pFus-faces) via the ventral occipital fasciculus (for a review, see Grill-Spector
199 et al. 2018; Takemura et al. 2016). Moreover, the IPS has a vital role in spatial representations
200 (Colby & Goldberg 1999; Fitzgerald et al. 2012; Goodale & Milner 1992), and the spatial
201 relationships between the eyes, nose, and mouth are important for face perception (e.g., Tsao &
202 Livingstone 2008). Hoffman and Haxby (2000) revealed that both the FG and the IPS responded to
203 faces more than to control stimuli (scrambled pictures) in a face perception task. Thus, we
204 established the IPS ROIs by comparing the brain activity in response to faces vs scrambled faces in
205 the functional localization task using a similar procedure as that used for identifying the ventral
206 visual cortices ($p < .05$, α ~ .10). The average size of the left and right IPS ROI across all
207 participants was 110 and 113 voxels, respectively. The results of MVPA for the ventral visual cortex
208 and IPS were calculated by averaging the accuracy of the left and right ventral visual cortices and
209 left and right IPSs because there were no significant hemispheric differences in MVPA accuracy.
210   The second type of scan was a retinotopy scan. Three 6-min retinotopy scans were performed to
211 identify low-level and mid-level visual areas (Fig. 5). We used a standard phase-encoding method in
212 which the retinotopic stimulus consisted of the natural images (same as those used in the functional
213 localization scan) displayed within a wedge- or ring-shaped aperture traversing the visual field. The
214 details of the procedure have been described in previous publications (e.g., Yamamoto et al. 2012;
215 Yamashiro et al. 2014). Unfortunately, in the present study, we could not collect reliable retinotopic
216 mapping data for most of the participants, which is likely attributed to the small number of the scans
217 and/or participant fatigue; due to the time limits for use of the MRI scanner, we could only perform
218 three retinotopy scans after the main experiment when the participants were tired. Since the data
219 were mostly insufficient in size and quality, clear retinotopy maps were only obtained for two

220   participants from which we identified V1, V2, V3, and V3A/B. Based on AFNI's Talairach Atlas, V1,
221   V2, and V3 were defined as the regions along the calcarine sulcus (Brodmann's area (BA) 17), the
222   cuneus and lingual gyrus (BA 18) surrounding V1, and the cuneus and lingual gyrus surrounding V2,
223   respectively. We also defined V3A/B, considering V3A as the area near the transverse occipital
224   sulcus and V3B as the area lateral relative to V3A (for a review, see Wandell et al. 2007). The
225   average ROI sizes across participants were as follows: left/right V1 = 193/289 voxels, left/right V2 =
226   129/160 voxels, left/right V3 = 127/152 voxels, left/right V3A/B = 174/136 voxels. The MVPA
227   accuracy for the early visual cortices was calculated by averaging the left and right hemispheres
228   because no significant hemispheric differences were found.
229

Results

Behavioral results

232   In the VWM experiment, participants performed the delayed roughness discrimination task in
233   which they indicated whether the probe sphere had higher or lower roughness than the memorized
234   sample sphere. Data from one participant who did not understand the task were removed from the
235   analysis. Overall, participants performed well in this experiment: the mean accuracy was 68.04%,
236   which exceeded chance ($t(22) = 8.51$, $p < .001$, $r = .88$).
237

fMRI MVPA results

239   We analyzed data from all participants except for the removed one for the fMRI analysis. First, we
240   investigated the topographic relationship between the categorical processing visual areas in the
241   ventral visual pathway and roughness VWM. Specifically, we localized face-, scene-, object-, and
242   color-related areas in the ventral visual pathway and IPS. In the ventral visual pathway, the
243   face-related area was localized near the FG, in keeping with literature reporting that this region is
244   involved in face perception (McCarthy et al. 1997). The scene-related area corresponded to the
245   parahippocampal place area where scene information is believed to be processed (e.g., Epstein &
246   Kanwisher 1998). The object-related region appeared to correspond with the lateral occipital
247   complex (Malach et al. 1995), and the color-related region was identified between the face- and
248   scene-related areas (Lafer-Sousa et al. 2016). For each these areas, we averaged the MVPA accuracy
249   from 8–12 s following the start of each trial (Fig. 6). We found that the MVPA accuracies were
250   above chance in the face ROI of the ventral visual cortex and the IPS ROI. The face-related ventral
251   visual cortex had 54.86% MVPA accuracy, which significantly higher than chance ($t(22) = 2.18$, p
252    $< .05$, $r = .42$). In contrast, the MVPA accuracies of the scene-, object-, and color-related ventral
253   visual cortices were not significantly different from chance (51.38%, $t(22) = 0.45$, $p = .66$, $r = .10$;
254   53.15%, $t(22) = 0.88$, $p = .39$, $r = .18$; 50.51%, $t(22) = 0.18$, $p = .86$, $r = .04$). The IPS showed
255   54.64% accuracy, which exceeded chance ($t(22) = 2.28$, $p < .05$, $r = .44$). No statistical differences in

256 MVPA accuracies were found between the left and right hemispheres for all regions (face-related
257 ventral visual cortex: $t(22) = 1.77$, $p = .09$, $r = .35$; scene-related ventral visual cortex: $t(22) = 0.40$, p
258 $= .69$, $r = .09$; object-related ventral visual cortex: $t(22) = 0.02$, $p = .98$, $r = .01$; color-related ventral
259 visual cortex: $t(22) = 0.04$, $p = .97$, $r = .01$; and IPS: $t(22) = 0.94$, $p = .36$, $r = .20$).

260   Second, we examined whether the early visual cortex was involved in roughness VWM. We
261 anatomically defined V1, V2, V3, and V3A/B and calculated the MVPA accuracy for each area
262 during the delay period (Fig. 7). We found that the MVPA accuracies were not significantly different
263 from chance in all ROIs (V1: 51.74%, $t(22) = 0.67$, $p = .51$, $r = .14$; V2: 51.23%, $t(22) = 0.47$, p
264 $= .64$, $r = .10$; V3: 52.24%, $t(22) = 0.78$, $p = .44$, $r = .16$; V3A/B: 52.97%, $t(22) = 1.04$, $p = .31$, r
265 $= .22$). There were also no statistical differences in MVPA accuracies between the left and right
266 hemispheres in all regions (V1: $t(22) = 0.74$, $p = .47$, $r = .16$; V2: $t(22) = 1.56$, $p = .13$, $r = .03$; V3:
267 $t(22) = 1.10$, $p = .28$, $r = .23$; V3A/B: $t(22) = 0.64$, $p = .53$, $r = .13$).

268

Discussion

270   In this study, we examined whether visual image information represented in the early visual cortex
271 was involved in the maintenance of VWM representations of illumination-invariant visual properties.
272 If the maintenance of VWM representations of roughness is independent of visual properties that
273 substantially change appearance due to a change in illumination, visual image information in the
274 early visual cortex should not be required. Alternatively, if visual image information is involved in
275 maintaining stable illumination-invariant VWM representations of roughness (Ester et al. 2016;
276 Christophel et al. 2017), these representations should include image-based information in the early
277 visual cortex. To address this question, we focused on a single object surface property (i.e.,
278 roughness) and performed a delayed roughness discrimination task in which sample and probe
279 stimuli differed in illumination. By applying MVPA to brain activity in the ventral visual cortex, IPS,
280 and early visual cortex, we found that the ventral visual cortex and IPS, but not the early visual
281 cortex, contributed to roughness VWM. This result suggests that a stable roughness VWM
282 representation can be established without visual images features from the early visual cortex.

283

Comparison with previous studies on VWM

285   Our findings are not consistent with those of some neuroimaging studies on VWM. Previous studies
286 have reported that VWM stability increases with distributed functions over multiple regions (e.g.,
287 Christophel et al. 2017). Although some studies have shown that the IPS has an important role in the
288 maintenance of VSTM (e.g., Todd & Marois 2004), more recent studies have identified the early
289 visual cortex as another potential region involved in VWM maintenance. For example, in the delayed
290 orientation discrimination task used in Harrison and Tong (2009), participants had to memorize the
291 orientation of a sample Gabor patch and judge whether the test Gabor was rotated clockwise or

292   counterclockwise compared with the memorized sample. Christophel et al. (2012) used more complex

293   stimuli (i.e., color patterns) and conducted a delayed similarity detection task. In that task, participants

294   had to indicate which of two probe color patterns was similar to the memorized sample color pattern.

295   Two factors may have contributed to the discrepancies in findings between our study and other

296   published studies. First, differences in visual features can influence whether the early visual cortex is

297   involved in VWM. While previous studies on VWM used a Gabor patch, we focused on an object

298   surface property. Although the early visual cortex is involved in maintenance of simple visual features,

299   complex features are retained in high-level areas. Second, differences in visual images between the

300   memory phase and the discrimination phase in a delayed discrimination task can influence VWM

301   maintenance in the early visual cortex. In past studies, participants had to retain a cued sample visual

302   image in their VWM. Then, in the discrimination phase, participants had to judge the probe images

303   based on the sample visual image maintained in VWM. However, in day-to-day life we often

304   encounter visual images in illuminations and viewpoints that are different than those in which the

305   image was first seen. In these conditions, visual input from the novel illumination or viewpoint of a

306   previously-encountered stimulus can interfere with low-level representation in VWM, and the

307   robustness of VWM may be reduced. Therefore, maintenance of low-level information in the early

308   visual cortex may disrupt robust VWM representations. In these two factors, illumination-invariant

309   visual features and changes in visual images between the sample and probe stimuli are not mutually

310   exclusive, and either factor alone may disrupt VWM representation in the early visual cortex. This is a

311   matter that needs to be examined in a future study.

312   The results of our study expand on previous studies investigating viewpoint in scene recognition (e.g.,

313   Xiao et al. 2010) that suggest that high-level areas such as the IPS show a viewpoint-invariant

314   response. This study by Xiao et al. (2010) was inconclusive regarding the role of the early visual areas

315   in scene recognition because they only used univariate analysis. In general, univariate analysis is not

316   sufficiently sensitive to evaluate representation in a brain region, as evidenced by failures of univariate

317   analysis in locating VWM representation in the early visual cortex (cf. Harrison & Tong 2009). In this

318   respect, our findings with MVPA provide more convincing evidence that involvement of the early

319   visual cortex is not essential for retaining a stable VWM representation.

320   Our results could have also been affected by top-down processes in the human brain. Bettencourt and

321   Xu (2016) conducted a delayed orientation discrimination task, similar to Harrison and Tong (2009),

322   except that visual distractors were presented during the delay period. When visual distractors were

323   presented in a random trial, the orientation of a memorized Gabor patch was retained in the early

324   visual cortex and IPS. In contrast, when the presence of visual distractors was predictable, only the

325   IPS was involved in retaining the VWM representation. We built upon this finding in that the early

326   visual cortex was not related to VWM when the participants could predict not only the presence of

327   distractors but also environmental differences between a memorized sample stimulus and a probe

328 stimulus. Indeed, distribution of VWM representation in the human brain is altered depending on

329 task demand (Lee et al. 2013; for a review, see Lee & Baker 2016). A future study should examine the

330 top-down effect by manipulating the predictability of illumination change. If our results are based on

331 stimulus features alone, the early visual cortex should not be related to VWM irrespective of the

332 predictability of illumination changes. Alternatively, if a top-down factor influences the involvement

333 of the early visual cortex in VWM, the early visual cortex should contribute to VWM only when

334 illumination change is unpredictable.

335   More recently, Rademaker et al. (2019) employed a delayed-match-to-sample (DMTS) task and

336 showed that memorized orientation was not impeded by noise distractors. Conversely, behavioral

337 and memory reconstruction performance decreased in the presence of visual distractors, in contrast

338 to the findings of Bettencourt and Xu (2016). Rademaker et al. (2019) attributed this discrepancy to

339 difference in protocols, suggesting that the use of a single memory sample and continuous report

340 design rendered VWM maintenance more sensitive to visual distractors during behavioral

341 performance than that in the study by Bettencourt and Xu (2016). To account for distractor-resistant

342 VWM, Rademaker et al. (2019) proposed that the early visual cortex may represent the input during

343 VWM maintenance because different neuronal populations process sensory and memory

344 representations; however, this theory predicts that VWM representation in the early visual cortex

345 should have been observed in our study. This incongruity may be explained by differences in the levels

346 of visual features used in each study (i.e., low-level Gabor patches in Rademaker et al. (2019) and

347 high-level roughness renderings in the present study). Future research is needed to examine whether

348 roughness VWM information can be interpreted from brain activity in a DMTS task for roughness.

349

350 **Comparison with previous studies on material perception**

351   We showed that the ventral visual cortex, but not the early visual cortex, is involved in

352 illumination-invariant roughness representation in VWM. Although recent neuroimaging studies

353 have revealed that the ventral visual cortex plays an important role in material perception (Sun et al.

354 2015; Wada et al. 2014), the early visual cortex was also reported to be involved because material

355 information was perceived in a series of processes from low- to high-level areas. By examining the

356 role of the ventral visual cortex during maintenance in a VWM task, we were able to distinguish the

357 role of the ventral visual cortex from that of the early visual cortex in VWM for the object surface

358 feature of roughness in different illumination conditions.

359   Our results are consistent with past findings on material perception (Hiramatsu et al. 2011; Sun et al.

360 2015; Wada et al. 2014). Material properties are encoded in various brain regions, from the early

361 visual cortex to the ventral visual cortex. Although low-level visual features are needed for material

362 perception, they are not sufficient on their own to represent material properties (Hiramatsu et al.

363 2011). Once material perception is established, visual information in the early visual cortex may no

364 longer be needed. Fleming et al. (2003) demonstrated that humans could match object glossiness and
365 roughness between two spheres, even when these stimuli were rendered under different real-world
366 illuminations. Moreover, Tsuda and Saiki (2018) revealed that the constancy of glossiness and
367 roughness against illumination was also observed in VWM. These findings indicate that we can
368 extract surface properties even when low-level features such as color, contrast, and highlights of the
369 reflected illumination image (e.g., Chadwick & Kentridge 2015; Marlow et al. 2011) are lost because
370 of illumination changes.

371 A recent neuroimaging study showed that the ventral visual cortex was involved in VSTM for
372 material category. Otsuka and Saiki (2019) conducted image-based and material category-based
373 change detection tasks and found differences in brain activation in the ventral visual cortex between
374 these tasks. However, no previous studies have investigated brain processes of VWM for specific
375 material properties (e.g., roughness) that are involved with the material categorization (Fleming et al.
376 2013). The main reason for the lack of the research regarding VWM for material properties lies in
377 the difficulty of manipulating the stimuli (Fleming 2014; for a review, see Komatsu & Goda 2018).
378 In this study, we manipulated a roughness parameter accurately using computer graphics and
379 revealed that the ventral visual cortex was involved in VWM for roughness. Our finding expands on
380 that of Otsuka and Saiki (2019) in that the ventral visual cortex is related to VWM/VSTM for both
381 material properties and material category.

382

Conclusion
384 It has been shown that distributed brain regions, including the early visual cortex, form and
385 maintain stable VWM representations. However, to achieve a stable VWM representation for
386 illumination-invariant object properties, illumination-invariant representation may be formed
387 without the need for information from the early visual cortex to distinguish changes between sample
388 and probe stimuli. We performed a delayed roughness discrimination task and found that the ventral
389 visual cortex and IPS, but not the early visual cortex, were involved in roughness VWM. This
390 finding suggests that a stable VWM representation is not always accompanied by visual features
391 from the early visual cortex during maintenance, even in the absence of distractors.

392

References
394 Bettencourt KC, Xu Y (2016) Decoding the content of visual short-term memory under distraction in
395   occipital and parietal areas. Nat Neurosci 19:150–157. https://doi.org/10.1038/nn.4174
396 Cant JS, Arnott SR, Goodale MA (2009) fMR-adaptation reveals separate processing regions for the
397   perception of form and texture in the human ventral stream. Exp Brain Res 192:391–405.
398   https://doi.org/10.1007/s00221-008-1573-8
399 Chadwick AC, Kentridge RW (2015) The perception of gloss: a review. Vision Res 109:221–235.

https://doi.org/10.1016/j.visres.2014.10.026

Chang CC, Lin CJ (2011) LIBSVM: a library for support vector machines. ACM Trans Intell Syst Technol 2:1–27

Christophel TB, Hebart MN, Haynes JD (2012) Decoding the contents of visual short-term memory from human visual and parietal cortex. J Neurosci 32:12983–12989. https://doi.org/10.1523/JNEUROSCI.0184-12.2012

Christophel TB, Klink PC, Spitzer B, Roelfsema PR, Haynes JD (2017) The distributed nature of working memory. Trends Cogn Sci 21:111–124. https://doi.org/10.1016/j.tics.2016.12.007

Colby CL, Goldberg ME (1999) Space and attention in parietal cortex. Annu Rev Neurosci 22:319–349. https://doi.org/10.1146/annurev.neuro.22.1.319

Cox RW (1996) AFNI: software for analysis and visualization of functional magnetic resonance neuroimages. Comput Biomed Res 29:162–173. https://doi.org/10.1006/cbmr.1996.0014

Dale AM (1999) Optimal experimental design for event-related fMRI. Hum Brain Mapp 8:109–114

Debevec PE (1998) Rendering synthetic objects into real scenes: Bridging traditional and image-based graphics with global illumination and high dynamic range photography. Proc SIGGRAPH:189–198. https://doi.org/10.1145/280814.280864

Epstein R, Kanwisher N (1998) A cortical representation of the local visual environment. Nature 392:598–601. https://doi.org/10.1038/33402

Ester EF, Rademaker RL, Sprague TC (2016) How do visual and parietal cortex contribute to visual short-term memory? eNeuro 3: ENEURO.0041-16.2016. https://doi.org/10.1523/ENEURO.0041-16.2016

Fitzgerald JK, Swaminathan SK, Freedman DJ (2012) Visual categorization and the parietal cortex. Front Integr Neurosci 6:18. https://doi.org/10.3389/fnint.2012.00018

Fleming RW (2014) Visual perception of materials and their properties. Vision Res 94:62–75. https://doi.org/ 10.1016/j.visres.2013.11.004

Fleming RW, Dror RO, Adelson EH (2003) Real-world illumination and the perception of surface reflectance properties. J Vis 3:347–368. https://doi.org/10.1167/3.5.3

Fleming RW, Wiebel C, Gegenfurtner K (2013) Perceptual qualities and material classes. J Vis 13:9. https://doi.org/10.1167/13.8.9

Goodale MA, Milner AD (1992) Separate visual pathways for perception and action. Trends Neurosci 15:20–25. https://doi.org/10.1016/0166-2236(92)90344-8

Grill-Spector K, Weiner KS, Gomez J, Stigliani A, Natu VS (2018) The functional neuroanatomy of face perception: from brain measurements to deep neural networks. Interface Focus 8:20180013. https://doi.org/10.1098/rsfs.2018.0013

Harrison A, Jolicoeur P, Marois R (2010) "What" and "Where" in the intraparietal sulcus: an fMRI study of object identity and location in visual short-term memory. Cereb Cortex 20:2478–2485.

436   https://doi.org/10.1093/cercor/bhp314

437   Harrison SA, Tong F (2009) Decoding reveals the contents of visual working memory in early visual

438   areas. Nature 458:632–635. https://doi.org/10.1038/nature07832

439   Haynes JD, Rees G (2005) Predicting the orientation of invisible stimuli from activity in human

440   primary visual cortex. Nat Neurosci 8:686–691. https://doi.org/10.1038/nn1445

441   Hiramatsu C, Goda N, Komatsu H (2011) Transformation from image-based to perceptual

442   representation of materials along the human ventral visual pathway. Neuroimage 57:482–494.

443   https://doi.org/10.1016/j.neuroimage.2011.04.056

444   Hoffman EA, Haxby JV (2000) Distinct representations of eye gaze and identity in the distributed

445   human neural system for face perception. Nat Neurosci 3:80–84. https://doi.org/10.1038/71152

446   Just MA, Carpenter PA, Maguire M, Diwadkar V, McMains S (2001) Mental rotation of objects

447   retrieved from memory: A functional MRI study of spatial processing. J Exp Psychol Gen

448   130:493–504. https://doi.org/10.1037/0096-3445.130.3.493

449   Komatsu H, Goda N (2018) Neural mechanisms of material perception: quest on shitsukan.

450   Neuroscience 392:329–347. https://doi.org/10.1016/j.neuroscience.2018.09.001

451   Lafer-Sousa R, Conway BR, Kanwisher NG (2016) Color-biased regions of the ventral visual pathway

452   lie between face- and place-selective regions in humans, as in macaques. J Neurosci 36:1682–

453   1697. https://doi.org/10.1523/JNEUROSCI.3164-15.2016

454   Lee SH, Baker CI (2016) Multi-voxel decoding and the topography of maintained information during

455   visual working memory. Front Syst Neurosci 10:2. https://doi.org/10.3389/fnsys.2016.00002

456   Lee SH, Kravitz DJ, Baker CI (2013) Goal-dependent dissociation of visual and prefrontal cortices

457   during working memory. Nat Neurosci 16:997–999. https://doi.org/10.1038/nn.3452

458   Malach R, Reppas JB, Benson RR, Kwong KK, Jiang H, Kennedy WA, Ledden PJ, Brady

459   TJ, Rosen BR, Tootell RB (1995) Object-related activity revealed by functional magnetic

460   resonance imaging in human occipital cortex. Proc Natl Acad Sci USA 92:8135–8139.

461   https://doi.org/10.1073/pnas.92.18.8135

462   Marlow P, Kim J, Anderson BL (2011) The role of brightness and orientation congruence in the

463   perception of surface gloss. J Vis 11:16. https://doi.org/10.1167/11.9.16

464   McCarthy G, Puce A, Gore JC, Allison T (1997) Face-specific processing in the human fusiform

465   gyrus. J Cogn Neurosci 9:605–610. https://doi.org/10.1162/jocn.1997.9.5.605

466   Motoyoshi I, Nishida S, Sharan L, Adelson EH (2007) Image statistics and the perception of surface

467   qualities. Nature 447:206–209. https://doi.org/10.1038/nature05724

468   Otsuka S, Saiki J (2019) Neural correlates of visual short-term memory for objects with material

469   categories. Heliyon 5:e03032. https://doi.org/10.1016/j.heliyon.2019.e03032

470   Rademaker RL, Chunharas C, Serences JT (2019) Coexisting representations of sensory and

471   mnemonic information in human visual cortex. Nat Neurosci 22:1336–1344. https://doi.or

472   g/10.1038/s41593-019-0428-x

473   Saad ZS, Reynolds RC, Argall B, Japee S, Cox RW (2004) SUMA: an interface for surface-based

474   intra- and inter-subject analysis with AFNI. Proc IEEE Int Symp Biomed Imaging 2:1510–1513.

475   https://doi.org/10.1109/ISBI.2004.1398837

476   Sun HC, Ban H, Di Luca M, Welchman AE (2015) fMRI evidence for the processing of surface gloss

477   in human visual cortex. Vision Res 109:149–157. https://doi.org/10.1016/j.visres.2014.11.012

478   Takemura H, Rokem A, Winawer J, Yeatman JD, Wandell BA, Pestilli F (2016) A major human white

479   matter pathway between dorsal and ventral visual cortex. Cereb Cortex 26:2205–2214.

480   https://doi.org/10.1093/cercor/bhv064

481   Todd JJ, Marois R (2004) Capacity limit of visual short-term memory in human posterior parietal

482   cortex. Nature 428:751–754. https://doi.org/10.1038/nature02466

483   Todd JJ, Marois R (2005) Posterior parietal cortex activity predicts individual differences in vis

484   ual short-term memory capacity. Cogn Affect Behav Neurosci 5:144–155. https://doi.org/10.

485   3758/cabn.5.2.144

486   Tsao DY, Livingstone MS (2008) Mechanisms of face perception. Annu Rev Neurosci 31:411–437.

487   https://doi.org/10.1146/annurev.neuro.30.051606.094238

488   Tsuda H, Saiki J (2018) Constancy of visual working memory of glossiness under real-world

489   illuminations. J Vis 18:14. https://doi.org/10.1167/18.8.14

490   Ungerleider LG, Courtney SM, Haxby JV (1998) A neural system for human visual working memory.

491   Proc Natl Acad Sci USA 95:883–890. https://doi.org/10.1073/pnas.95.3.883

492   Wada A, Sakano Y, Ando H (2014) Human cortical areas involved in perception of surface glossiness.

493   Neuroimage 98:243–257. https://doi.org/10.1016/j.neuroimage.2014.05.001

494   Wandell BA, Dumoulin SO, Brewer AA (2007) Visual field maps in human cortex. Neuron 56:366–

495   383. https://doi.org/10.1016/j.neuron.2007.10.012

496   Ward GJ (1994) The RADIANCE lighting stimulation and rendering system. Comput Graphics

497   28:459–472. https://doi.org/10.1145/192161.192286

498   Xiao C, McNamara TP, Qin S, Mou W (2010) Neural mechanisms of recognizing scene con

499   figurations from multiple viewpoints. Brain Res 1363:107–116. https://doi.org/10.1016/j.br

500   ainres.2010.09.068

501   Xing Y, Ledgeway T, McGraw PV, Schluppeck D (2013) Decoding working memory of stimulu

502   s contrast in early visual cortex. J Neurosci 33:10301–10311. https://doi.org/10.1523/JNEU

503   ROSCI.3754-12.2013

504   Xu Y, Chun MM (2006) Dissociable neural mechanisms supporting visual short-term memory for

505   objects. Nature 440:91–95. https://doi.org/10.1038/nature04262

506   Yamamoto H, Fukunaga M, Takahashi S, Mano H, Tanaka C, Umeda M, Ejima Y (2012) In

507   consistency and uncertainty of the human visual area loci following surface-based registr

508   ation: probability and entropy maps. Hum Brain Mapp 33:121–129. https://doi.org/10.100

509   2/hbm.21200

510   Yamashiro H, Yamamoto H, Mano H, Umeda M, Higuchi T, Saiki J (2014) Activity in early visual

511   areas predict interindividual differences in binocular rivalry dynamics. J Neurophysiol
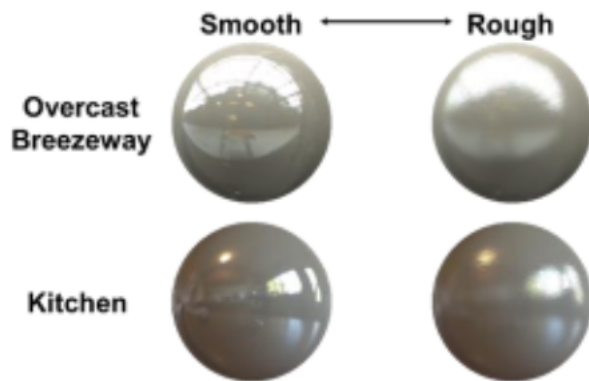
512   111:1190–1202. https://doi.org/10.1152/jn.00509.2013

513   **Fig. 1** Computer-generated three-dimensional spheres used as sample stimuli. The surface appearance
514   of the sample spheres was set at one of two levels of roughness with jitters.
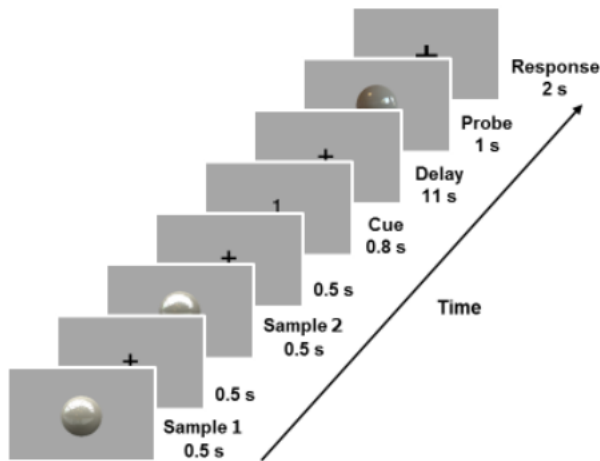
516   **Fig. 2** Sample trial of the delayed roughness discrimination task. The two samples spheres were of
517   different roughness. After an 11-s delay following the memorization cue, a probe sphere was
518   presented, and participants were asked to indicate whether the probe had higher or lower roughness
519   than the memorized sample sphere.
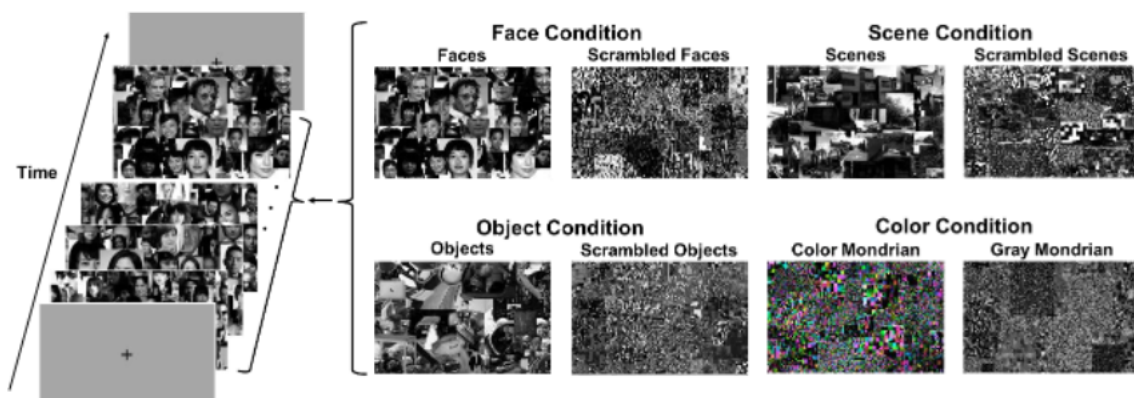
521   **Fig. 3** Sample block of the functional localization scan. Within each block, collages of natural
522   images belonging to a single block condition were presented for sequentially 0.5 s each.
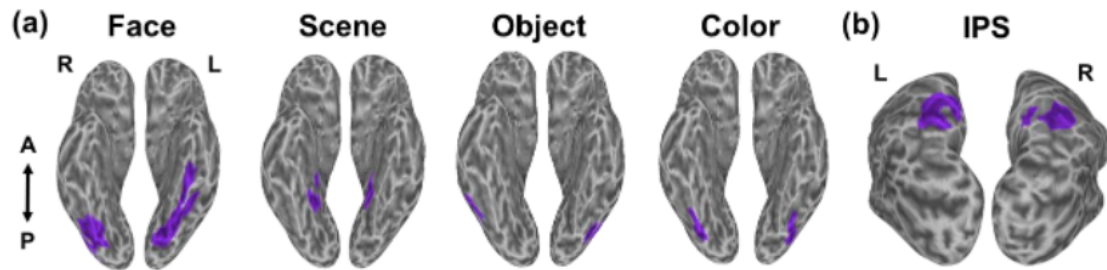
523

17

524
525 **Fig. 4** Representative example of left and right extruded brain surfaces. We defined regions of interest
526 based on the functional localization scans. **a** Left and right ventral visual cortices were identified,
527 which are related to face-, scene-, object-, and color-processing. **b** Left and right intraparietal sulci
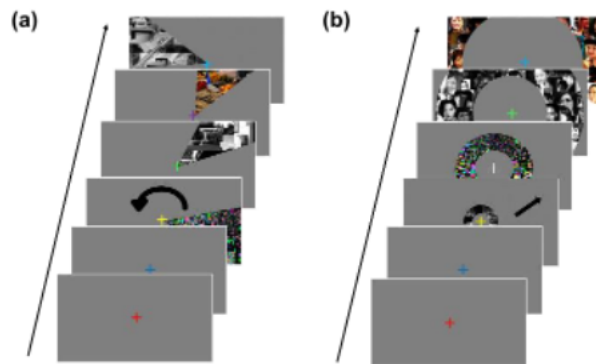528 (IPSs) were localized based on the face condition in the functional localization scans.

529
530 **Fig. 5** Sample retinotopy scans. **a** A counterclockwise polar angle wedge run (CCW run) during
531 which a 45° wedge rotated counterclockwise around the entire screen at 12 Hz for 60 s. The CCW
532 run was conducted twice. **b** An expanding ring run (EXP run) during which a ring expanded across
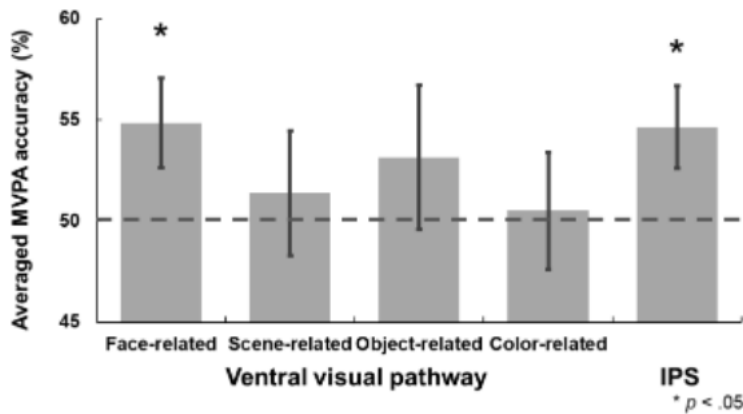533 the entire screen for 60 s. The EXP run once was conducted once.

534
535   **Fig. 6** Averaged multi-voxel pattern analysis (MVPA) accuracy for the dissociation of roughness
536   (rough or smooth) during the period from 8–12 s following the start of each trial. The gray dotted line
537   signifies the chance level of accuracy (50%) and the error bars show standard error. (IPS: intraparietal
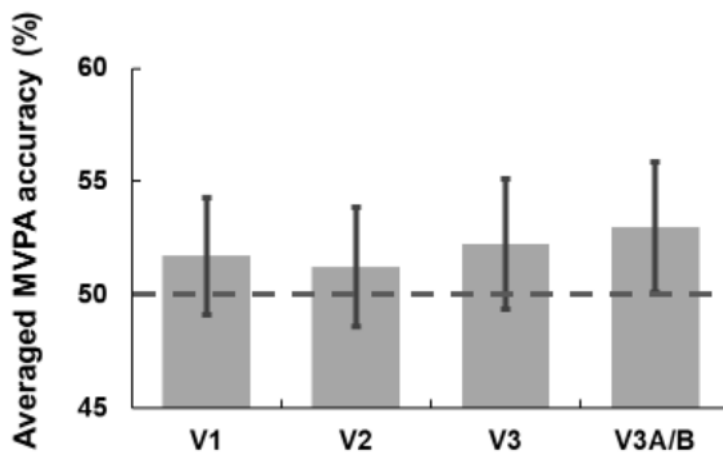538   sulcus).

539
540   **Fig. 7** Averaged multi-voxel pattern analysis (MVPA) accuracy in the early visual cortex during the
541   delay period. The gray dotted line signifies the chance level of accuracy (50%) and the error bars show
542   standard error.